Molecular Ecology

WILEY

MOLECULAR ECOLOGY

ORIGINAL ARTICLE

Hybrid Zone Analysis Using Coalescent-Based Estimates of Introgression and Migration in Plateau Fence Lizards (*Sceloporus tristichus*)

Adam D. Leaché[1,2] | Hayden R. Davis[1,2] | Sonal Singhal[3]

[1]Department of Biology, University of Washington, Seattle, Washington, USA | [2]Burke Museum of Natural History and Culture, University of Washington, Seattle, Washington, USA | [3]Department of Biology, California State University-Dominguez Hills, Carson, California, USA

Correspondence: Adam D. Leaché (leache@uw.edu)

Received: 22 January 2025 | **Revised:** 7 May 2025 | **Accepted:** 16 May 2025

Handling Editor: Josephine Pemberton

Funding: This project was supported by Division of Environmental Biology grants to A.D.L. (NSF-SBS-2023723) and S.S. (NSF-SBS-2023979).

Keywords: cline analysis | hybridization | multispecies coalescent | phylogeography | systematics

ABSTRACT

Coalescent modelling of hybrid zones can provide novel insights into the historical demography of populations, including divergence times, population sizes, introgression proportions, migration rates and the timing of hybrid zone formation. We used coalescent analysis to determine whether the hybrid zone between phylogeographic lineages of the Plateau Fence Lizard (*Sceloporus tristichus*) in Arizona formed recently due to human-induced landscape changes, or if it originated during Pleistocene climatic shifts. Given the presence of mitochondrial DNA from another species in the hybrid zone (Southwestern Fence Lizard, *S. cowlesi*), we tested for the presence of *S. cowlesi* nuclear DNA in the hybrid zone as well as reassessed the species boundary between *S. tristichus* and *S. cowlesi*. No evidence of *S. cowlesi* nuclear DNA is found in the hybrid zone, and the paraphyly of both species raises concerns about their taxonomic validity. Introgression analysis placed the divergence time between the parental hybrid zone populations at approximately 140 kya and their secondary contact and hybridization at approximately 11 kya at the end of the Pleistocene. Introgression proportions estimated for hybrid populations are correlated with their geographic distance from parental populations. The multispecies coalescent with migration provided significant support for unidirectional migration moving from south to north, which is consistent with spatial cline analyses that suggest a slow but steady northward shift of the centre of the hybrid zone over the last two decades. When analysing hybrid populations sampled along a linear transect, coalescent methods can provide novel insights into hybrid zone dynamics.

1 | Introduction

Hybrid zones are geographic areas where genetically distinct populations produce offspring with a mixture of traits from the parental populations (Harrison 1993; Gompert et al. 2017). Naturally occurring hybrid zones provide important insights into the evolutionary processes of speciation, gene flow, and species boundaries (Harrison and Larson 2014). Typically, researchers study hybrid zones using spatial and/or genomic cline methods. Spatial clines describe the geographic characteristics of a hybrid zone, including the location of the centre of the hybrid zone (cline centre), the width of the hybrid zone (cline width), and when multiple loci are compared, differential introgression among marker types (Barton and Hewitt 1985; Szymura and Barton 1986). Genomic clines leverage large numbers of loci from across the genome to provide insights into differential

introgression among genes or chromosomal regions (Gompert and Buerkle 2011). Another tool for the analysis of hybrid zones is the multispecies coalescent (MSC), which can infer the historical demography of populations including their divergence times and population sizes (Rannala and Yang 2003). New MSC models that include introgression (Jiao et al. 2021; Ji et al. 2023) or migration (Flouri et al. 2023) can add critical information to hybrid zone studies such as the timing of hybrid zone formation, introgression rates from parental to hybrid populations, and migration rates. In this study, we apply both spatial clines and MSC models to a Plateau Fence Lizard (*Sceloporus tristichus*) hybrid zone to test hypotheses regarding the age of the hybrid zone and extent of introgression and migration between populations.

The *S. tristichus* hybrid zone is in Arizona's Colorado Plateau at an ecological transition zone between Great Basin Conifer Woodlands in the south and Grassland habitats in the north; this transition zone facilitates hybridization between morphologically and ecologically distinctive grassland and woodland populations (Leaché and Cole 2007). Interestingly, in addition to the introgression dynamics that connect these distinctive populations of *S. tristichus* together, mitochondrial DNA (mtDNA) from the Southwestern Fence Lizard (*S. cowlesi*) is also found in the hybrid zone (Leaché and Cole 2007). Haplotypes from both species are found in hybrid populations, which have a maximum uncorrected sequence divergence of 10.6% (Leaché and Cole 2007). However, the potential for co-introgression of mtDNA and nuclear DNA (e.g., Sloan et al. 2017) remains untested. Thus, we take a phylogeographic approach to test the species boundary between *S. tristichus* and *S. cowlesi* using range-wide geographic sampling of both species. Phylogenetic and population structure analyses are used to assess whether the mtDNA species boundary is supported by nuclear data and to determine if *S. cowlesi* nuclear DNA occurs in the hybrid zone.

After confirming that the hybrid zone only consists of *S. tristichus* nuclear DNA, we use coalescent inference and spatial clines to better understand this hybrid zone. We first seek to estimate when the hybrid zone formed. The canyon ecotone habitats that support hybridization may have formed as recently as the 1890s with the onset of intensive cattle grazing, which mediated the northward expansion of juniper trees into former grasslands (Archer 1994; Abruzzi 1995). Alternatively, palynological evidence suggests that juniper expansion in the American Southwest began at least several thousand years earlier (Davis and Turner 1986; Miller and Wigand 1994). To test these alternative hypotheses explaining the formation of the hybrid zone, we use the MSC with introgression (MSC-I), which can estimate the introgression time between populations (Figure 1a).

Temporal sampling combined with spatial cline analysis over multiple decades has provided evidence that the centre of the cline is moving to the north (Leaché and Cole 2007; Leaché et al. 2017). A comparison of specimens collected in the 1970s and 2002 shows changes in the frequency of a chromosome inversion polymorphism (e.g., a distinctive pericentric inversion polymorphism on chromosome seven) that is consistent with the hypothesis of northward hybrid zone movement (Leaché and Cole 2007). Also, DNA sequence comparisons of samples collected in 2002 and 2012 provide evidence that the mtDNA cline is displaced from the nuclear cline and maintaining an introgression distance of approximately 3 km. Both the nuclear and mtDNA clines have shifted north by approximately 2 km over this time interval, which equals roughly 10 lizard generations (Leaché et al. 2017). In this study, we use a new replicate of transect samples from 2022 and a spatial cline analysis to test the prediction that the hybrid zone has continued to shift to the north over the last decade. Because the hybrid zone has moved north through time, we might expect to also see higher migration rates from south to north. We use the MSC with migration (MSC-M; Figure 1b) to test this expectation by estimating bi-directional migration rates between the parental populations.

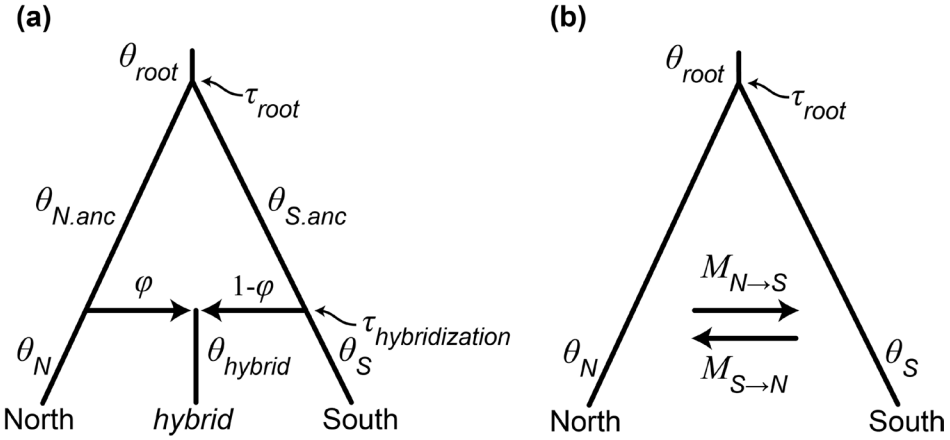

FIGURE 1 | Multispecies coalescent models used to estimate population demographic parameters in the hybrid zone. (a) The introgression model (MSC-I) includes nine parameters: six population sizes (θ_N, θ_S, θ_{hybrid}, $\theta_{N.anc}$, $\theta_{S.anc}$, θ_{root}), one divergence time (τ_{root}), one hybridization time ($\tau_{hybridization}$), and one introgression probability (φ) defined as the proportion of the hybrid population genome originating from one of the parental populations (the proportion of the genome originating from the other population is $1-\varphi$). Parameters for the MSC-I were estimated separately for each hybrid sample site. (b) The migration model (MSC-M) includes six parameters: three population sizes (θ_N, θ_S, θ_{root}), one divergence time (τ_{root}), and two migration rates ($M_{N\to S}$, $M_{S\to N}$). Migration rate is the expected number of migrants from the donor population to the recipient population per generation.

TABLE 1 | Summary of the *Sceloporus tristichus* hybrid zone transect sites over 10-year intervals using replicate sampling. Distance (km) is from the northernmost locality (Holbrook). Numbers in parentheses are sample sizes. Nuclear DNA values are ancestry proportions (Q) estimated using ADMIXTURE, which show the fraction of ancestry from the northern population under a $K=2$ model. mtDNA frequencies are the fraction of samples from a site that group with the northern clade versus the southern clade (haplotypes grouping with western *S. tristichus* or *S. cowlesi* are not considered).

		Nuclear DNA			Mitochondrial DNA		
Site name	**Distance**	**2002**	**2012**	**2022**	**2002**	**2012**	**2022**
Holbrook	0	0.98 (9)	1.00 (20)	1.00 (7)	0.92 (13)	1.00 (20)	1.00 (7)
Fivemile Wash	8.3	1.00 (8)	0.89 (20)	0.99 (11)	1.00 (8)	1.00 (9)	1.00 (9)
Washboard Wash	14.5	1.00 (9)	0.98 (20)	0.99 (10)	1.00 (11)	1.00 (18)	1.00 (6)
Woodruff	22.6	1.00 (4)	0.98 (20)	1.00 (9)	1.00 (9)	1.00 (12)	1.00 (1)
Canoncito	29.3	0.89 (24)	0.83 (40)	0.87 (10)	0.72 (25)	1.00 (18)	1.00 (5)
Sevenmile Draw	35.2	0.29 (8)	0.23 (20)	0.22 (10)	0.83 (12)	0.80 (10)	0.83 (6)
Snowflake	42.7	0.00 (7)	0.02 (19)	0.01 (10)	0.00 (5)	0.00 (14)	0.50 (8)
Show Low	63.5	0.00 (9)	0.00 (20)	0.00 (11)	0.00 (12)	0.00 (20)	0.00 (11)

2 | Materials and Methods

2.1 | Hybrid Zone Sampling

We collected 79 samples from the hybrid zone in 2022 at the eight transect sites sampled in 2002 and 2012 (Tables 1 and S1). The sampling transect extends 63.5 km from grassland habitat in the north (Holbrook) to juniper woodland habitat in the south (Show Low). Canyon ecotones that connect these habitats are where lizards with mixed genotypes, intermediate phenotypes, and heteromorphic pairs of chromosomal inversions are found (Leaché and Cole 2007). We compared the 2022 transect to 95 samples collected in 2002 (Leaché and Cole 2007) and 179 samples collected in 2012 (Leaché et al. 2017). Scientific collecting was approved by the State of Arizona Game and Fish Department (Permit #SP843452). Animal research was approved by the University of Washington Office of Animal Welfare (IACUC #4367–03).

2.2 | Mitochondrial DNA Analysis

To determine the frequency of *S. tristichus* and *S. cowlesi* haplotypes at each hybrid zone sample site, we conducted a phylogenetic analysis of mtDNA sequences. We extracted genomic DNA from tissue samples using salt extraction (Aljanabi and Martinez 1997). We amplified and sequenced the mitochondrial *ND1* protein-coding gene (969 bp) using standard PCR methods (Leaché and Cole 2007). We aligned new *ND1* sequences with previously published data, which included additional hybrid zone samples, broad-scale sampling of *S. cowlesi* and *S. tristichus*, and other closely related species (*S. cautus*, *S. consobrinus*, *S. occidentalis*, *S. undulatus*, *S. virgatus* and *S. woodi*; Table S2). New mtDNA sequences are deposited in GenBank (Accessions PQ901620–PQ901697; PV462017–PV462129). The final alignment containing 755 sequences is available on Dryad (doi: https://doi.org/10.5061/dryad.47d7wm3rz).

We estimated a maximum likelihood (ML) phylogeny using IQ-TREE v.1.6.12 (Nguyen et al. 2015) with 1000 ultrafast bootstraps (Hoang et al. 2018) and the ModelFinder option to evaluate 286 nucleotide substitution models (Kalyaanamoorthy et al. 2017). The final tree presented is a consensus tree from the bootstrap replicates (with default settings "-bb 1000"). The Bayesian information criterion (BIC) was used to select the best-fit model, since this criterion outperforms others in identifying the true model (Li et al. 2025).

2.3 | Nuclear Data Collection

We collected nuclear data using double digestion restriction site associated DNA sequencing (ddRADseq; Peterson et al. 2012). We followed the same library preparation methods used in a previous study of the hybrid zone (Leaché et al. 2017). Briefly, we double-digested genomic DNA with restriction enzymes SbfI and MspI, ligated barcodes, adapters, and unique molecular identifiers (UMIs), and then pooled samples for size selection and PCR amplification of libraries. Samples were sequenced on one lane with an Illumina NovaSeq 6000 (100 bp single-end reads) at the QB3 facility at UC Berkeley.

2.4 | Nuclear Data Assembly

We assembled the Illumina reads using ipyrad v.0.7.3 (Eaton and Overcast 2020). The assembly was guided using a reference genome of *S. tristichus* from an individual originating from the northern parental population (Bedoya and Leaché 2021). We de-multiplexed samples using their unique barcode and adapter sequences, and sites with Phred quality scores under 99% (Phred score = 33) were changed into 'N' characters and reads with ≥10% N's were discarded. After the removal of the 6 bp restriction site overhang, the 6 bp barcode, and 8 bp UMI, the samples were clustered using a sequence similarity threshold of 90%. Additional filtering included discarding clusters that

had low coverage (< 10 reads), excessive undetermined or heterozygous sites (> 4), or too many haplotypes (> 2 for diploids). We assembled all 335 hybrid zone samples collected from 2002, 2012 and 2022 together to ensure that shared loci were obtained. The demultiplexed sequences are available on the NCBI Sequence Read Archive (PRJNA1211730). The assembled data output files are available on Dryad (doi: https://doi.org/10.5061/dryad.47d7wm3rz).

2.5 | Phylogeographic Analysis of *S. tristichus* and *S. cowlesi* Using Nuclear Data

Mitochondrial DNA from *S. cowlesi* is found in the *S. tristichus* hybrid zone, so we tested for evidence of nuclear introgression from *S. cowlesi* into *S. tristichus* as well. To do so, we assembled a phylogeographic dataset (ddRADseq data) of samples from *S. tristichus* and *S. cowlesi*. We then analysed these data using phylogenetic and population genetic methods to provide broader geographic and evolutionary contexts for understanding the composition of the hybrid zone in relation to both species.

A total of 56 samples were included in the phylogeographic analysis, with species assignments determined using their mtDNA-based phylogenetic placement (Figure S1 and Table S3). The samples were obtained from four sources: (1) we downloaded 35 samples from the NCBI Sequence Read Archive for a previous study of *S. tristichus* (Bedoya and Leaché 2021), (2) we included eight hybrid zone samples from the 2022 transect (one sample from each hybrid zone site), (3) we collected new data for 10 samples used in a previous study of the species group (Leaché and Reeder 2002), which included a sample of *S. consobrinus* to root the phylogeny, and (4) we collected new data for three samples loaned from the University of Texas at El Paso Herpetology Collection.

Library preparations and data collection for the new samples followed the same protocols as described above. We processed the data using ipyrad with the same reference genome as the hybrid zone assembly. For the phylogenetic analysis, we exported a concatenated data matrix containing all loci in phylip format and excluded sites with more than 10% missing data. For population structure analysis, we exported a VCF file and used VCFtools v.0.1.16 (Danecek et al. 2011) to sample biallelic loci, apply a minor allele frequency threshold of 0.01, exclude sites with more than 50% missing data, and sample one random SNP per locus. The demultiplexed sequences are available on the NCBI Sequence Read Archive (PRJNA1211730), and the data files are available on Dryad (doi: https://doi.org/10.5061/dryad.47d7wm3rz).

We estimated a ML phylogeny using IQ-TREE with the same approach as described above for the mtDNA analysis. We estimated population structure using ADMIXTURE v.1.3.0 (Alexander et al. 2009) for K values ranging from $K = 1$–8. The model with the lowest CV error was selected as the best-fit model (Alexander et al. 2009). We performed 10 replicate runs for each K value using random starting seeds. Admixture bar plots were generated with StructuRly v.0.1.0 (Criscuolo and Angelini 2020).

2.6 | Population Structure of the Hybrid Zone

We estimated population structure and ancestry proportions for the hybrid zone using ADMIXTURE. The data were filtered using VCFtools to sample biallelic loci, apply a minor allele frequency threshold of 0.01, and to retain one SNP per locus. We determined the optimal number of clusters (K) by comparing the cross-validation (CV) error scores for analyses with K values ranging from 1 to 8. The K value with the lowest CV error was selected as the best model. We performed 4 replicate runs for each K value using random starting seeds. Population structure bar plots were generated with StructuRly. After selecting the optimal model ($K = 2$) we ran separate ADMIXTURE analyses for each transect time series to estimate the ancestry proportion (Q) for each sample site. The estimated Q values (Table 1) were used in spatial cline analyses (see below).

We also used the R package gghybrid (Bailey 2024) to estimate genome-wide hybrid index h and its uncertainty for each sample. The hybrid index represents the proportion of the genome originating from parental reference populations: Holbrook (northern) and Show Low (southern). This is similar to the Q value estimated with ADMIXTURE when $K = 2$ (Bailey 2024). Under this model, each allele is treated independently, and the probability that an individual allele originated from one of the source populations depends on the frequency of the allele in each source population and the hybrid index of the sample (Buerkle 2005). We followed the recommended analysis procedures and ran the chain for 3000 iterations with a 1000-step burn-in period (Bailey 2024).

2.7 | Cline-Fitting Analysis

We performed cline-fitting analyses using the R package hzar (Derryberry et al. 2014). To identify the optimal cline model, we used the Akaike information criterion (AIC) to compare 10 different models against a null model that assumes no cline. The cline models combine two parameter settings: the trait interval (two settings: fixed to 0 and 1 versus estimated values) and exponential tail-fitting (five settings: none fitted; left only; right only; mirror tails; tails estimated separately). After selecting the optimal model, we performed ML cline fitting separately for each sample period (2002, 2012, 2022). Nuclear clines were estimated using Q values estimated from ADMIXTURE for each sample site (Table 1). MtDNA clines were estimated using the proportion of haplotypes grouping with the northern *S. tristichus* clade versus the southern clade (Table 1). Haplotypes occurring in the hybrid zone that grouped with the western clade of *S. tristichus* or *S. cowlesi* were ignored. Cline parameters of interest included cline centre (measured as distance in kilometres from the northern population) and cline width (kilometres). Parameter uncertainty was estimated using 2-log-likelihood (2LL) support limits.

2.8 | Multispecies Coalescent With Introgression or Migration

We used the multispecies coalescent with introgression (MSC-I) in the program BPP v.4.7 (Rannala and Yang 2003;

Flouri et al. 2020) to estimate the timing of hybridization and the proportion of introgression from parental populations into the hybrid zone. The hybrid zone model includes three populations: two parental populations that diverge at τ_{root} and later hybridise at time $\tau_{hybridization}$ leading to a hybrid population (Figure 1a). This model is described as a hybrid speciation model whereby populations come into contact to form a hybrid species (Flouri et al. 2020), and we consider this model a good representation for the *S. tristichus* hybrid zone, where two populations have come into contact to form a hybrid population. The introgression probability (φ) is the proportion of the hybrid population genome that is derived from the parent population. A limitation of this model is that it does not account for any introgression that occurs between the initial hybridization event and the present day, nor for potential introgression from unsampled populations (here, other hybrid zone localities).

We conducted six separate MSC-I analyses to estimate $\tau_{hybridization}$ and $\varphi_{North \to x}$ for each of the hybrid populations while holding the parental populations constant (north = Holbrook; south = Show Low). These analyses used the 2022 transect data assembled with no missing data ($n = 738$ loci), since this dataset contained the most loci. Allowing no missing data ensured that the results using different hybrid populations were comparable by maintaining the same loci across all six analyses. We used gamma priors for population sizes (θ) and the root age (τ_{root}), with the prior mean G(2, 1000) = 0.002, which are close to empirical estimates derived from the study system. The prior for introgression probability (φ) used a beta distribution ~ beta(1,1), which provides a flat prior distribution. We used a burn-in of 40,000 iterations, and took 400,000 samples, sampling every 2 iterations. Each analysis was repeated four times with different starting seeds. Convergence was assessed by calculating the potential scale reduction factor (PSRF) using the R package CODA (Plummer et al. 2006) with values close to 1 indicating convergence. Posterior distributions from the four separate runs were combined to calculate parameter values and the effective sample size (ESS). The hybridization time ($\tau_{hybridization}$) and root age (τ_{root}) were converted to absolute time assuming a lizard-specific substitution rate of 3.17^{-9} mutations/site/year (Bergeron et al. 2023) and a one-year generation time (Tinkle and Dunham 1986).

To estimate the amount of gene flow between the parental populations without the influence of the hybrid samples, we estimated their bi-directional migration rates using the MSC with migration (MSC-M; Flouri et al. 2023). The two-population model includes six parameters: two migration rates, three population sizes (two populations and their ancestor), and one divergence time (Figure 1b). The migration rate $M = mN$ is measured in the expected number of migrants from the donor population to the recipient population per generation; N is the (effective) population size of the recipient population, and m is the proportion of immigrants in the recipient population (from the donor population) every generation, with time moving forward (Flouri et al. 2023). The migration rate prior used a gamma distribution G(1,10) with mean 1/10 = 0.1 migrant individuals per generation (1 migrant individual every 10 generations). All other priors, run settings, and convergence diagnostics matched those used in the MSC-I analyses described above.

The statistical significance of gene flow was evaluated using Bayes factors (BF) calculated with the Savage-Dickey density ratio (Ji et al. 2023). The test compares BF_{10} in support of the gene flow model (H_1) over the null model of no gene flow (H_0). The test was considered significant if $BF_{10} > 20$. We used a cut-off of $\varphi > 0.01$ (1% introgression) for the introgression model and a cut-off of $M > 0.01$ (1 migrant every 100 generations) for the migration model (Ji et al. 2023).

3 | Results

3.1 | Mitochondrial DNA Analysis

We conducted a phylogenetic analysis of the *ND1* gene to calculate the frequency of mtDNA haplotypes found at each site in the hybrid zone. The *ND1* alignment contains 775 sequences with 371 parsimony-informative sites. Model selection using the BIC selected the TIM + F + I + G4 model, which is a transition model (TIM) with empirical base frequencies (F), a parameter that allows for a proportion of invariable sites (I), and among-site rate variation using a discrete gamma model with 4 rate categories (G4). The mtDNA phylogeny places the hybrid zone samples into the four distinct clades defined in previous studies; three of these clades belong to *S. tristichus* and one belongs to *S. cowlesi* (Figure 2a). A detailed version of the mtDNA genealogy with bootstrap support values and tip labels is provided in Supporting Information (Figures S2–S4).

The northern *S. tristichus* haplotypes are found in high frequency (97%) in the northernmost population (Holbrook) and decline to 0% in the south (Show Low), while the southern *S. tristichus* haplotypes show the opposite pattern (Table 2). The western *S. tristichus* haplotypes do not form a cline, but instead are found at relatively low frequency (2%–26%) in three of the southern populations. The *S. cowlesi* haplotypes enter the hybrid zone from the east and are found in the middle of the hybrid zone from Fivemile Wash to Snowflake with relatively high frequencies in the north (57% and 77%; Table 2). All four haplotypes occur together in three populations: Canoncito, Sevenmile Draw, and Snowflake (Table 2).

3.2 | Phylogeographic Analysis of *S. tristichus* and *S. cowlesi* Using Nuclear Data

The phylogeographic dataset contains a total of 2549 ddRAD-seq loci with 5915 variable sites. Concatenating the loci for phylogenetic analysis and filtering out sites with > 10% missing data produced an alignment with 78,003 base pairs and 532 parsimony-informative sites. The filtered VCF file for population structure analysis contained 1741 SNPs.

Phylogenetic analysis of the concatenated data using IQ-TREE selected the TPM3u + F + R2 model using the BIC. The phylogeny does not support the monophyly of *S. tristichus* or *S. cowlesi* as currently defined based on their mtDNA assignments (Figures 3a and S5). The base of the phylogeny contains a paraphyletic group of samples from across New Mexico, while samples from Utah, western Colorado, and Wyoming are nested

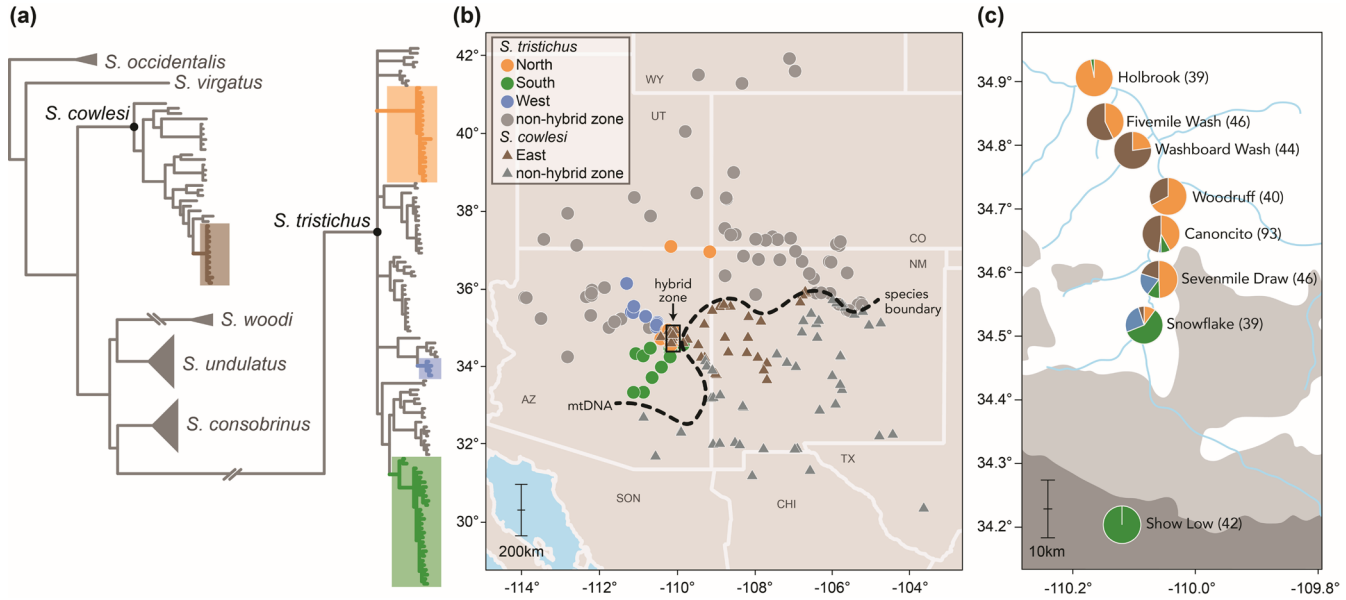

FIGURE 2 | Phylogeny and geographic distributions of *Sceloporus tristichus* and *S. cowlesi* in the Southwestern United States based on mitochondrial DNA (mtDNA). (a) Phylogenetic relationships based on the *ND1* gene estimated using maximum likelihood (rooted with *S. occidentalis*). The four mtDNA clades that are found in the hybrid zone are colour-coded. (b) Geographic distributions of *S. tristichus* (circles) and *S. cowlesi* (triangles), the distributions of the clades detected in the hybrid zone, and the mtDNA species boundary (dashed line). (c) Pie-charts showing mtDNA haplotype frequencies in the hybrid zone. Sample sizes are shown in parentheses. The shaded areas show habitat distributions of Petran Montane Conifer Forest (dark grey), Great Basin Conifer Woodland (light grey), and Great Basin Grassland (unshaded/white). [Colour figure can be viewed at wileyonlinelibrary.com]

TABLE 2 | Frequency of *Sceloporus tristichus* and *S. cowlesi* mtDNA haplotypes at hybrid zone localities aggregated across three time points (2002, 2012 and 2022). Haplotypes from *S. cowlesi* enter the hybrid zone from the east and are found at all sites except for the parental populations in Holbrook and Show Low.

		S. tristichus			*S. cowlesi*
Site name	***N***	**North**	**South**	**West**	
Holbrook	39	0.97	0.03	0.0	0.0
Fivemile wash	46	0.43	0.0	0.0	0.57
Washboard wash	44	0.23	0.0	0.0	0.77
Woodruff	40	0.68	0.0	0.0	0.33
Canoncito	93	0.42	0.08	0.02	0.48
Sevenmile draw	46	0.50	0.10	0.20	0.20
Snowflake	39	0.10	0.59	0.26	0.05
Show low	42	0.0	1.0	0.0	0.0

within a clade composed primarily of samples from Arizona (Figures 3a and S5).

The optimal population structure model for the phylogeographic dataset is a 3-population model ($K=3$; Figure S6). The geographic distributions of these populations do not match the mtDNA species boundary (Figure 3). Inspection of the next best models ($K=2$ and $K=4$) also fails to show any correspondence to the mtDNA species boundary (Figure 3). If we assume that the southern New Mexico population cluster represents *S. cowlesi* (ignoring issues related to paraphyly and admixture), then there is no evidence that *S. cowlesi* nuclear DNA is found near the hybrid zone under any of these population models (Figure 3).

3.3 | Nuclear Data Assembly

The reference-based assembly of the 335 hybrid zone samples resulted in 4030 loci containing 6934 variable sites. Filtering the VCF file for population structure analysis retained 1830 SNPs. A summary of the assembly is provided in Table S4.

3.4 | Population Structure of the Hybrid Zone

The best-fit population structure model based on a comparison of CV error scores is a two-population model ($K=2$; Figure S7). For each transect sampling time, the ancestry proportions show a steep transition from northern ancestry to southern ancestry in the centre of the hybrid zone (Table 1). Models assuming higher K values ($K=3$ and $K=4$) maintain a clear separation between the parental populations while adding additional structure to the middle of the hybrid zone (Figure S8).

To calculate the proportion of the genome originating from each of the parental populations, we estimated the hybrid index h of each sample. The hybrid index plot shows a transition from northern to southern ancestry with greater northern ancestry in Woodruff, Washboard Wash, Fivemile Wash and Canoncito, and greater southern ancestry in Sevenmile Draw

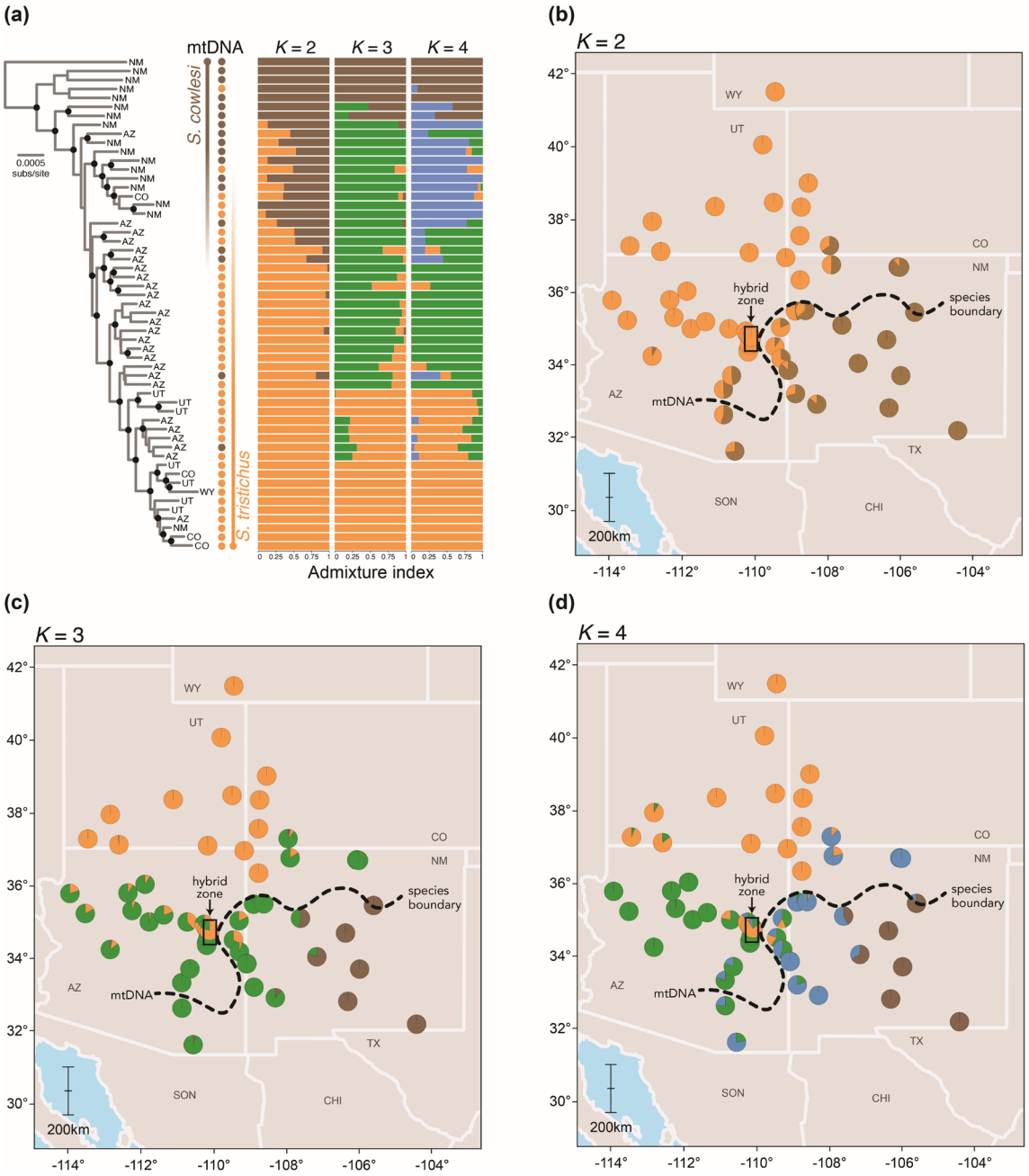

FIGURE 3 | Phylogeography of *Sceloporus tristichus* and *S. cowlesi* in the Southwestern United States based on nuclear DNA. (a) Phylogenetic relationships estimated with the concatenated ddRADseq loci using maximum likelihood. mtDNA species assignments are shown for each sample. Phylogenetic tips are labelled by their geographic origin (State), using abbreviations shown on the maps in (b–d). Based on the $K = 3$ analysis in (c), *S. cowlesi* nuclear DNA (brown) does not approach the hybrid zone, which is made up of the nuclear DNA of southern (green) and northern (orange) populations of *S. tristichus*. The barplots show SNP-based admixture results for models assuming $K = 2$, $K = 3$, and $K = 4$ populations. The geographic distributions of these populations are in (b) $K = 2$, (c) $K = 3$ (best-fit model), and (d) $K = 4$. Pie-charts on the maps show individual admixture proportions. [Colour figure can be viewed at wileyonlinelibrary.com]

and Snowflake (Figure 4a). A histogram of hybrid index values shows a deficit of F1 hybrids at $h = 0.5$, and instead suggests that most samples represent late-stage backcrosses (Figure 4b).

3.5 | Cline-Fitting Analysis

Spatial cline-fitting analyses were conducted to test the prediction that the hybrid zone is shifting to the north by comparing ML cline centre estimates between decades. Cline-fitting model selection using the AIC favoured a simple two-parameter model that combines fixed trait intervals ($p_{min} = 0$, $p_{max} = 1$) without exponential tail fitting (tails = none). This model was supported by both the nuclear and mtDNA data (Table S5). Movement of the hybrid zone is supported by the northward shift in cline centres in the nuclear data (Table 3). However, although the ML cline centre estimates show directional movement, the magnitude of change is not significant when considering the overlap in

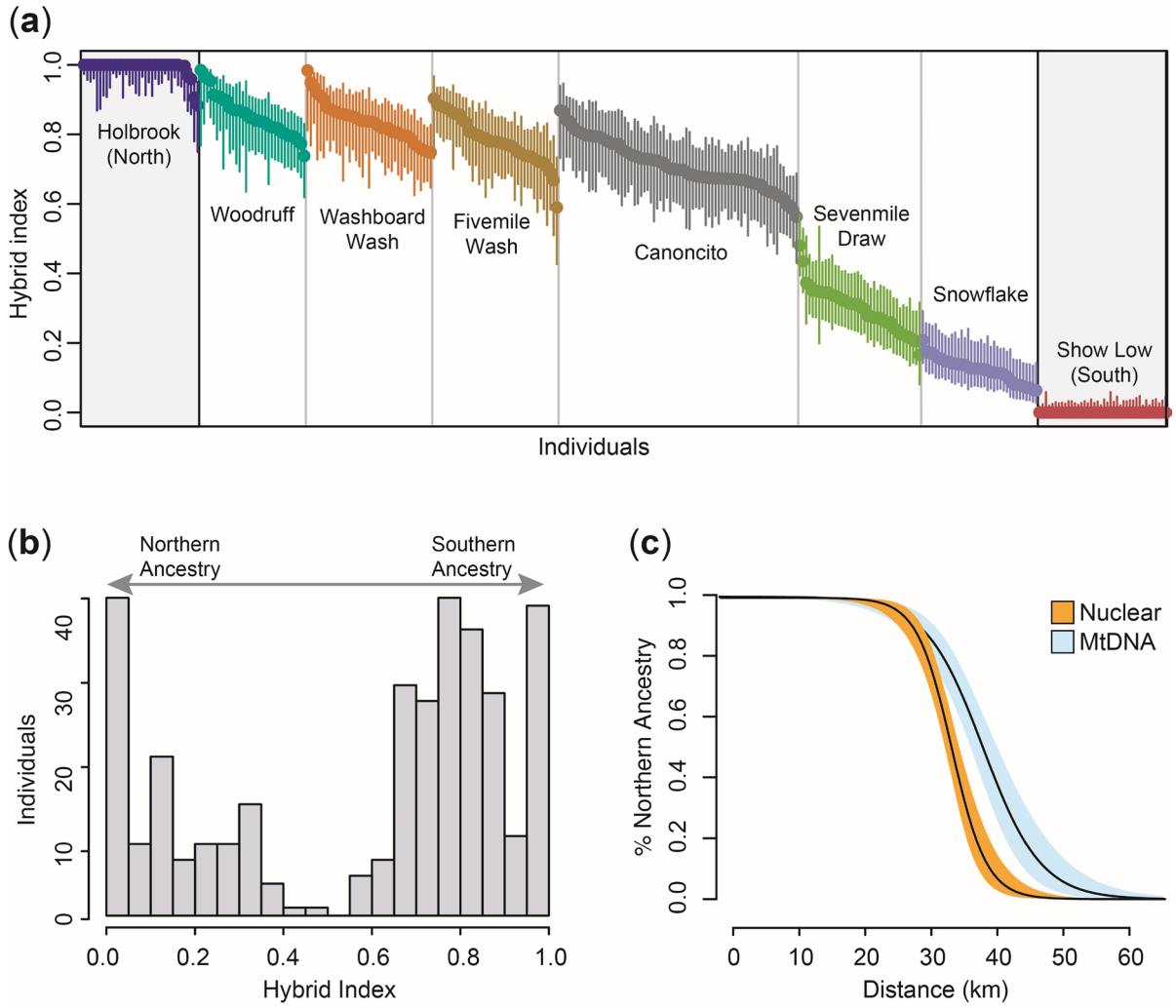

FIGURE 4 | Patterns of hybridization and introgression for the *Sceloporus tristichus* hybrid zone. (a) Hybrid index plot shows decreasing northern ancestry along the hybrid zone. The posterior mode (dot) and 95% credible interval (error bars) is shown for each sample. The points are ordered by population mean and then individual estimates. (b) Histogram of hybrid index values across all eight populations shows a high frequency of late-stage backcrosses. (c) Nuclear and mtDNA clines (with 95% confidence intervals). [Colour figure can be viewed at wileyonlinelibrary.com]

TABLE 3 | Temporal comparison of cline centres and widths for the *Sceloporus tristichus* hybrid zone. Cline movement measures the change in cline centre compared to the previous transect sampling year. Distances are in kilometres, and the 2-log-likelihood support limits (2LL) are in parentheses (minimum–maximum).

Data	Year	Cline centre	Cline movement	Cline width
Nuclear	2002	33.67 (31.60–36.78)	—	9.37 (5.42–18.28)
Nuclear	2012	33.05 (30.98–35.49)	+0.62 km	17.07 (12.10–24.86)
Nuclear	2022	32.85 (30.29–35.49)	+0.20 km	9.58 (5.40–18.18)
MtDNA	2002	37.79 (33.41–44.40)	—	27.65 (17.10–46.41)
MtDNA	2012	35.64 (35.19–38.99)	+2.15 km	1.27 (0.09–9.11)
MtDNA	2022	42.30 (38.11–48.66)	−6.66 km	14.03 (5.97–32.45)

2LL support limits (Table 3). Cline centres for mtDNA data are shifted to the south of the nuclear cline centres for each transect sample year; while the mtDNA cline moved in the same direction as the nuclear DNA cline in the interval 2002–2012 (north) it showed the opposite change (south) in the interval 2102–2022 (Table 3). Cline width estimates range from approximately 9–17 km for the nuclear data, while the mtDNA cline widths are relatively more variable, ranging from approximately 1–27 km

TABLE 4 | Demographic parameters for the *Sceloporus tristichus* hybrid zone estimated using the multispecies coalescent with introgression (MSC-I). For each hybrid population (x), the introgression probability ($\varphi_{\text{North}\rightarrow x}$) is the proportion of the hybrid population genome originating from the northern parental population (Holbrook). The proportion of the genome originating from the southern parental population ($\varphi_{\text{South}\rightarrow x}$) is 1-$\varphi_{\text{North}\rightarrow x}$ (not shown). The hybridization time ($\tau_{\text{hybridization}}$) and root age ($\tau_{\text{root}}$) are converted to units of thousands of years (kya) assuming a lizard-specific substitution rate of 3.17^{-9} mutations/site/year. Bayesian posterior distributions are summarised across four separate analyses by their mean and 95% HPD (in parentheses).

Hybrid pop (x)	$\varphi_{\text{North}\rightarrow x}$	$\tau_{\text{hybridization}}$	τ_{root}
Fivemile wash	0.726 (0.65–0.80)	8.86 (3.2–14.8)	141.98 (114.8–168.5)
Washboard wash	0.738 (0.66–0.82)	10.57 (3.2–18.6)	143.85 (115.5–172.6)
Woodruff	0.808 (0.72–0.89)	10.71 (3.8–18.3)	145.55 (118.9–172.6)
Canoncito	0.658 (0.58–0.74)	6.82 (1.9–12.6)	140.89 (114.8–166.9)
Sevenmile draw	0.304 (0.22–0.40)	15.97 (6.3–25.6)	147.44 (119.9–175.4)
Snowflake	0.131 (0.07–0.20)	10.65 (2.8–19.2)	154.99 (124.6–185.2)

(Table 3). Clines that show the displacement between the nuclear and mtDNA data are shown in Figure 4c.

3.6 | Multispecies Coalescent With Introgression or Migration

To estimate the timing of hybridization and the introgression probabilities from the parental populations into the hybrid zone, we conducted six separate analyses using the MSC-I (Figure 1a). Convergence diagnostics suggest that the analyses sampled from similar posterior distributions (Table S6). Across all six analyses, the gene flow model (H_1) is favoured over the no gene flow model (H_0) at a cut-off of $\varphi > 0.01$ with $BF_{10} > 20$ (Table S7). Introgression probabilities (φ) from the northern population (Holbrook) into each hybrid population decline as the geographic distance from the northern population increases; conversely, φ from the southern population (Show Low) into each hybrid population increases along this same gradient. The estimates for $\varphi_{\text{North}\rightarrow x}$ range from ~0.81 in the northern hybrid zone locations to as low as ~0.13 in the south (Table 4). The MSC-I contains two parameters related to time (Figure 1a), including the divergence time of the parental populations (τ_{root}) and hybridization event ($\tau_{\text{hybridization}}$). Estimates for τ_{root} vary for each analysis, but generally overlap with 95% highest posterior density (HPD) ranging from 114 to 185 kya (Table 4). The estimates for $\tau_{\text{hybridization}}$ are an order of magnitude younger with the most recent estimate at 6.82 kya (95% HPD = 1.9–12.6 kya) for the population closest to the centre of the hybrid zone (Canoncito; Table 4). A southern population, Sevenmile Draw, provides the oldest $\tau_{\text{hybridization}} = 15.97$ kya (95% HPD = 6.3–25.6 kya).

To estimate the migration rate between the parental populations, we used the MSC-M (Figure 1b). The gene flow model (H_1) is favoured for $M_{\text{South}\rightarrow\text{North}}$, but the no gene flow model (H_0) is favoured for $M_{\text{North}\rightarrow\text{South}}$ ($BF_{10} = 1.82$; Table S7). The unidirectional migration rate is estimated as $M_{\text{South}\rightarrow\text{North}} = 0.314$ (95% HPD = 0.17–0.46) or approximately 0.3 migrants per generation, or 3 migrants every 10 generations (Table 5). The divergence time estimated under the MSC-M is $\tau_{\text{root}} = 238.7$ kya (95% HPD = 160.9–318.9 kya; Table 5), which is relatively older but overlapping with the 95% HPD estimates of the MSC-I (Table 4).

TABLE 5 | Demographic parameters for the parental populations in the *Sceloporus tristichus* hybrid zone estimated using the multispecies coalescent with migration (MSC-M). Migration rate (M) is the expected number of migrants from the donor population to the recipient population per generation. A Bayes factor test rejects the migration rate $M_{\text{North}\rightarrow\text{South}}$ in favour of a no gene flow model (Table S7). The divergence time (τ_{root}) is converted to units of thousands of years (kya) assuming a lizard-specific substitution rate of 3.17^{-9} mutations/site/year. Bayesian posterior distributions are summarised across four separate analyses by their mean and 95% HPD.

Parameter	Mean	95% HPD
θ_{North}	0.00182	0.00133–0.00234
θ_{South}	0.00436	0.00345–0.00533
θ_{Ancestor}	0.00170	0.00117–0.00222
τ_{root}	238.7 kya	160.9–318.9 kya
$M_{\text{North}\rightarrow\text{South}}$	0.0365	0.000–0.105
$M_{\text{South}\rightarrow\text{North}}$	0.3139	0.170–0.456

4 | Discussion

4.1 | Phylogeography and Systematics of *S. tristichus* and *S. cowlesi*

The *Sceloporus tristichus* hybrid zone is complex because it involves a different species; *S. cowlesi*'s geographic range abuts the hybrid zone (Figure 2). Both previous and current analyses show that *S. cowlesi* mtDNA has introgressed into the *S. tristichus* hybrid zone (Figure 2). However, this introgression appears restricted to just the mitochondrial genome (Figure 3). Broad scale phylogeographic analyses find no evidence for *S. cowlesi* nuclear DNA near the hybrid zone. Further, samples within the hybrid zone are best described by a two-population

model (Figure S7), each of which corresponds to a parental *S. tristichus* population.

Given this, we analysed the *Sceloporus tristichus* hybrid zone using a two-population model, finding that both nuclear and mtDNA data show sharp transitions in frequencies in the middle of the hybrid zone (Table 1). Analysing these data in a spatial framework with cline-fitting analysis shows the steepness of the clines (Figure 4c) and pinpoints the centre of the hybrid zone to approximately 30–34 km south of Holbrook. The hybrid index analysis provides a visualisation of the cline that also supports a sharp transition in population ancestry (Figure 4a) and provides information about the relatively high abundance of late-stage backcross samples in comparison to F1 individuals (Figure 4b). Finally, the introgression probabilities obtained for each hybrid population using the MSC-I illustrate the clinal nature of the hybrid zone by showing a clear pattern of increased introgression with geographic proximity, with the largest change occurring between Canoncito and Sevenmile Draw (Table 4). The large shift in the genetic profiles of these populations is seen repeatedly by the shift in introgression probabilities measured with the MSC-I (Table 4), the change in ancestry proportions (Table 1), and the cline-fitting analyses (Figure 4).

Discordance between mtDNA and nuclear loci, either at the level of discordant spatial clines or conflicting phylogenies, is important to describe since these data are often used to delimit species. *Sceloporus cowlesi* and *S. tristichus* were delimited using mtDNA (Leaché and Reeder 2002); however, the broad scale phylogeographic patterns estimated using nuclear data do not match the mtDNA species boundary (Figure 3). The nuclear data support at least three populations, and none of them have a geographic boundary that coincides with the mtDNA species boundary (Figure 3). Instead of supporting discrete population boundaries as expected for independent evolutionary lineages, these population boundaries appear 'fuzzy' with admixed samples situated between them, suggesting that they are not species (Figure 3).

The nuclear phylogeny does not support the monophyly of *S. tristichus* or *S. cowlesi*, and the asymmetric shape of the base of the tree makes it a challenging framework from which to guide an updated taxonomy (Figures 3a and S5). A minimum of six separate lineages diverge in succession at the base of the phylogeny that are mostly (but not exclusively) attributable to *S.* "*cowlesi*" based on their mtDNA species assignments. A revised taxonomy that prioritises monophyly would require many new species. A new taxonomy with many species could be tailored to fit the phylogeny, but it would not match the population structure results, which support fewer groups (Figure 3). An alternative solution is to synonymize these taxa. *Sceloporus cowlesi* was described by Lowe and Norris (1956) as a subspecies of *S. undulatus* endemic to White Sands, New Mexico, whereas *Sceloporus tristichus* was first described by Edward D. Cope (in Yarrow 1875) with a type locality of Taos, Taos County, New Mexico. If this solution is adopted, then *S. tristichus* is the valid name based on the principle of priority. A formal taxonomic treatment of this study system that considers additional populations and morphological data is forthcoming.

4.2 | Assumptions of the Introgression and Migration Models

Coalescent analyses of divergence times typically only provide estimates for species and/or population splitting events, while the MSC-I adds a parameter for the timing of introgression upon secondary contact (Figure 1a). The estimated timing of secondary contact and introgression in the *S. tristichus* hybrid zone is approximately 10 kya, which is an order of magnitude younger than the divergence between the parental populations (Table 4). The *S. tristichus* hybrid zone has been hypothesized to result from anthropogenic disturbance. While we hypothesize that these disturbances are one factor leading to hybrid zone movement, these results suggest the hybrid zone more likely originated at the end of the Pleistocene, as populations expanded from glacial refugia (Table 4).

The MSC-I assumes that introgression is constant among the sampled loci (Flouri et al. 2020), but differences in both recombination rate and selection strength can cause introgression to vary across the genome (Martin and Jiggins 2017). Genome-wide variability in introgression rates has been documented using the MSC-I in *Anopheles* mosquitoes (Flouri et al. 2023) and *Heliconius* butterflies (Thawornwattana et al. 2023), which both show considerable variation in introgression rates across chromosome arms. Because our ddRADseq sampling across the genome is sparse, we cannot determine if the *S. tristichus* genome shows evidence for differential introgression across the genome. That said, a genomic region of interest in *S. tristichus* is the large pericentric inversion polymorphism on chromosome seven (Leaché and Cole 2007; Bedoya and Leaché 2021). Recombination is typically reduced within inversions because crossover events within inversions lead to imbalanced chromosomes (Kirkpatrick 2010). Reduced recombination can then lead to reduced introgression for multiple reasons—one of which is that reduced recombination means that inversions can more easily capture two or more alleles that are locally adapted to the environment (Martin et al. 2019). Inversions thus provide a selective advantage, resulting in reduced introgression (Faria et al. 2019).

In addition to the assumption of constant introgression, other assumptions of the MSC-I could influence our interpretation of the hybrid zone. The simplified MSC-I that we used only includes two parental and one hybrid population (Figure 1a), which makes it simple to implement and easy to interpret. However, this model does not fully capture hybrid zones, in which the populations spanning the zone are connected via migration and gene flow. Adding more hybrid populations to the MSC-I would be intractable because it would greatly increase the number of model parameters and thus computational demands. It is possible to estimate the rates and directions of migration events between multiple hybridising populations using MIGRATE-N (Beerli and Felsenstein 2001), but this model does not account for the phylogeny or the history of population divergence events. The phylogenetic framework used in the MSC-I enables the estimation of divergence times and introgression times. Finally, the introgression probabilities estimated by the MSC-I assume a single pulse of introgression at the time of secondary contact. Most conceptions of hybrid zones assume continuous gene flow and introgression as parentals move into the hybrid zone and hybrids mate

over generations. An alternative model that assumes constant migration throughout the duration of the population history is implemented in the MSC-M, but this model does not estimate the timing of secondary contact (Flouri et al. 2023).

4.3 | Hybrid Zone Dynamics

We describe the clinal nature of a moving hybrid zone in *S. tristichus* using three replicate transect samples collected over two decades. In many ways, the characteristics of this hybrid zone fit the common tension zone model (Key 1968), which assumes that hybrid zones are maintained by a balance between selection against hybrids and dispersal into the hybrid zone and that parentals have higher fitness than hybrids (Barton and Hewitt 1985). The *S. tristichus* hybrid zone is situated at a habitat ecotone, which, while not required by the tension zone model, is true for some presumed tension zones (Endler 1977). When a hybrid zone is restricted to an ecotone, any environmental or climatic changes that result in movement of the ecotone could cause a shift in the location of the hybrid zone (Taylor et al. 2015). Temporal sampling has documented hybrid zone movement in numerous plant and animal species at both contemporary (Buggs 2007) and historical times (Wielstra 2019), including studies of lizards (Hillis and Simmons 1986; Okamoto et al. 2024). A unique benefit of the *S. tristichus* study system is the ability to leverage temporal sampling to measure how the centre and width of the hybrid zone changes through time (Table 3). Nuclear data suggest that the centre of the cline is shifting to the north despite the relatively short duration between sampling intervals (10 years = ~10 generations), but these small shifts in cline centre are not significant (Table 3). However, the mtDNA cline from 2022 does not support this pattern, largely due to the detection of northern haplotypes at one southern sample site (Snowflake; Table 1).

A null model for any hybrid zone is neutral diffusion, in which there are no barriers to gene flow. As populations freely exchange genes, the cline widens over time as a function of dispersal rate. Here, we can use the estimates of the hybrid zone age to test the plausibility of this null model for the *S. tristichus* hybrid zone. Under neutral diffusion, cline width is given by:

$$w = \sqrt{2\pi} \times \sigma \times \sqrt{t}$$

where w is the cline width, σ is the standard deviation of the distance between parents and their offspring, and t is the time since secondary contact (Endler 1977). Time since secondary contact $= t_{hybridization}$ (11,000 years or ~ 11,000 lizard generations; Table 4) and $\sigma = 0.16\ km / \sqrt{gen}$ (inferred from a congeneric species *S. grammicus*; Sites et al. 1995). Thus, under a model of neutral diffusion, the predicted cline width is 40 km, which is more than four times greater than what we see in this system (cline width ~ 9 km; Table 3).

Because neutral diffusion is improbable, the hybrid zone between *S. tristichus* populations is more likely maintained by environmentally mediated selection and/or selection against hybrids (Endler 1977; Barton and Gale 1993). The *S. tristichus* populations occupy distinct habitats and have corresponding eco-morphologies–the northern and southern populations are found in woodlands and grasslands respectively, and the southern population is both smaller and darker than the northern population (Leaché and Cole 2007). The hybrid zone between these populations maps to the ecotone between them. Together, this evidence suggests that the hybrid zone is likely partially maintained by environmentally mediated selection.

Predictions from the tension zone model can be used to better understand the plausibility that the hybrid zone is maintained by selection against hybrids. Given cline width and a measure of dispersal, and assuming that assortative mating is weak, the strength of selection against hybrids can be estimated using the equation:

$$s* = 8 \times (\sigma / w)^2$$

Again, using the $\sigma = 0.16\ km / \sqrt{gen}$ and an average nuclear cline $w = 9$ km (Table 3), selection against hybrids is only 0.2%. However, chromosome seven contains a large pericentric inversion between these populations (Leaché and Cole 2007; Bedoya and Leaché 2021). While the role this inversion plays in local adaptation or reproductive barriers remains unclear, cline width at the inversion is much narrower than at the rest of the nuclear genome (1.5 km vs. 9 km; Table 3; Leaché and Cole 2007) and selection is much stronger (~9%). Thus, if selection against hybrids is maintaining this hybrid zone, this selection is likely relatively weak and heterogeneous across the genome. Indeed, as is true of many hybrid zones where both assortative mating and selection against hybrids is weak to moderate, the hybrid zone is dominated by backcrosses relative to F1s (Jiggins and Mallet 2000).

Whatever forces are maintaining this hybrid zone, they are strong enough to preserve the genetic integrity of the parental populations. Inside the hybrid zone, our results suggest extensive admixture and introgression (Table 1; Figure 4). Outside of the hybrid zone, the parental populations are separated by ~60 km and show limited levels of unidirectional gene flow ($M_{South \rightarrow North} = 0.314$; Table 5). This hybrid zone thus acts both as a geographic border between these two populations and a relatively impermeable barrier to gene flow (McEntee et al. 2020).

What then do these results tell us about the species status of the two *S. tristichus* populations? The two populations of *S. tristichus* that meet in the hybrid zone are estimated to have diverged near the end of the Pleistocene (Tables 4–5), which is much younger than the multimillion-year divergences seen among recognised species in the group (Leaché et al. 2016). Further, although they have distinctive phenotypes and a chromosomal inversion, they only have modest levels of genetic differentiation (mean $F_{ST} = 0.09$; weighted $F_{ST} = 0.23$). Thus, despite these differences and some evidence of reproductive barriers between them, these populations appear to be relatively early in their diversification trajectory.

4.4 | Comparison of Lizard Hybrid Zones

A recent meta-analysis identified 12 other lizard hybrid zones for which cline dynamics have been estimated (McEntee et al. 2020).

The *S. tristichus* hybrid zone has a few notable similarities and differences to these systems. First, the pattern of discordant mtDNA-nDNA clines is common across lizard systems. In eight out of ten lizard hybrid zones with both mtDNA and nuclear cline width estimates, nuclear clines are wider, with a median width 1.6 times greater than that of mtDNA clines. Although the pattern has varied over time, the most recent transect data from the *S. tristichus* hybrid zone indicate that the mtDNA cline is approximately 1.5 times wider than the nuclear DNA cline. Additionally, in all six hybrid zones with available cline centre data, mtDNA clines were not coincident with nuclear DNA clines. In many cases, the offset was substantially greater than the ~3 km observed in *S. tristichus*; for example, in *Podarcis muralis*, mtDNA and nDNA cline centres are separated by 50 km.

These results highlight that patterns of introgression often differ between nuclear and mitochondrial data. This is perhaps expected, given the unique biology of the mtDNA (Toews and Brelsford 2012; Ballard and Whitlock 2004). For example, mtDNA has a lower effective population size than nDNA, which can increase the role of genetic drift on this locus; genetic drift tends to narrow clines (Polechová and Barton 2011). Further, if species show sex-biased dispersal—as occurs in some lizard species (Li and Kokko 2019), this could either increase or decrease effective dispersal at the maternally inherited mtDNA relative to the nuclear genome, thus affecting clinal patterns (Endler 1977; Currat et al. 2008). In addition to the impacts from drift and dispersal, local adaptation of mtDNA haplotypes and mito-nuclear incompatibilities could serve as selective forces that impact mtDNA introgression.

Second, cline widths in the *S. tristichus* hybrid zone are relatively wide, especially compared to other hybrid zones with similar dispersal levels. Of the 12 other systems, three have inferred cline widths greater than this system. In another *Sceloporus* hybrid zone involving chromosomal races of *S. grammicus*, the hybrid zone is much narrower (less than a kilometre). This comparison highlights that selection is relatively weak in the *S. tristichus* system.

Finally, temporal sampling has revealed hybrid zone movement in at least two other systems, including *Pholidobolus* lizards in Ecuador (Hillis and Simmons 1986) and *Gekko* geckos in Japan (Okamoto et al. 2024). In both cases—as well as in *S. tristichus*—hybrid zone movement is thought to result from anthropogenic effects like habitat modification and invasive species, a hypothesis proposed to explain movement in other hybrid zones (Buggs 2007; Taylor et al. 2015). Given the dynamic range shifts occurring in many species within increasingly human-altered environments, we anticipate that temporal sampling of additional hybrid zones will reveal further cases of hybrid zone movement, as observed in *S. tristichus*. Continued monitoring will be critical for understanding the evolutionary consequences of these shifting contact zones.

Author Contributions

A.D.L. designed the study. A.D.L. and H.R.D. conducted fieldwork. H.R.D. collected ddRADseq data. A.D.L. and S.S. conducted analyses. All authors contributed to the text and approved the final manuscript.

Acknowledgements

We thank A. Carvalho, S. Wikramanayake, L. N'Diaye for help with fieldwork. We thank two anonymous reviewers and the AE for their helpful comments and suggestions. We thank the Arizona Game and Fish Department for issuing scientific collecting permits (LIC #SP843452). This project was supported by grants to A.D.L. (NSF-SBS-2023723) and S.S. (NSF-SBS-2023979).

Conflicts of Interest

The authors declare no conflicts of interest.

Data Availability Statement

Mitochondrial DNA sequences: Genbank accessions PQ901620–PQ901697 and PV462017–PV462129. Nuclear ddRADseq data: NCBI SRA Accession PRJNA1211730. Final data assemblies, analysis files, and scripts are available on the Dryad Digital Repository: https://doi.org/10.5061/dryad.47d7wm3rz. Additional supporting information may be found in the online version of the article at the publisher's website.

References

Abruzzi, W. S. 1995. "The Social and Ecological Consequences of Early Cattle Ranching in the Little Colorado River Basin." *Human Ecology* 23: 75–98.

Alexander, D. H., J. Novembre, and K. Lange. 2009. "Fast Model-Based Estimation of Ancestry in Unrelated Individuals." *Genome Research* 19: 1655–1664.

Aljanabi, S. M., and I. Martinez. 1997. "Universal and Rapid Salt-Extraction of High Quality Genomic DNA for PCR-Based Techniques." *Nucleic Acids Research* 25, no. 22: 4692–4693.

Archer, S. 1994. "Woody Plant Encroachment Into Southwestern Grasslands and Savannah: Rates, Patterns, and Proximate Causes." In *Ecological Implications of Livestock Herbivory in the West*, edited by M. Vavra, W. Laycock, and R. Pieper, 13–68. Society for Range Management.

Bailey, R. I. 2024. "Bayesian Hybrid Index and Genomic Cline Estimation With the R Package Gghybrid." *Molecular Ecology Resources* 24: e13910.

Ballard, J. W., and M. C. Whitlock. 2004. "The Incomplete Natural History of Mitochondria." *Molecular Ecology* 13: 729–744.

Barton, N. H., and K. S. Gale. 1993. "Genetic Analysis of Hybrid Zones." In *Hybrid Zones and the Evolutionary Process*, 13–45. Oxford University Press.

Barton, N. H., and G. M. Hewitt. 1985. "Analysis of Hybrid Zones." *Annual Review of Ecology, Evolution, and Systematics* 16: 113–148.

Bedoya, A. M., and A. D. Leaché. 2021. "Characterization of a Pericentric Inversion in Plateau Fence Lizards (*Sceloporus tristichus*): Evidence From Chromosome-Scale Genomes." *G3 (Bethesda, Md.)* 11: jkab036.

Beerli, P., and J. Felsenstein. 2001. "Maximum Likelihood Estimation of a Migration Matrix and Effective Population Sizes in *n* Subpopulations by Using a Coalescent Approach." *Proceedings of the National Academy of Sciences* 98: 4563–4568.

Bergeron, L. A., S. Besenbacher, J. Zheng, et al. 2023. "Evolution of the Germline Mutation Rate Across Vertebrates." *Nature* 615: 285–291.

Buerkle, C. A. 2005. "Maximum-Likelihood Estimation of a Hybrid Index Based on Molecular Markers." *Molecular Ecology Notes* 5: 684–687.

Buggs, R. J. A. 2007. "Empirical Study of Hybrid Zone Movement." *Heredity* 99: 301–312.

Criscuolo, N. G., and C. Angelini. 2020. "StructuRly: A Novel Shiny App to Produce Comprehensive, Detailed and Interactive Plots for Population Genetic Analysis." *PLoS One* 15: e0229330.

Currat, M., M. Ruedi, R. J. Petit, and L. Excoffier. 2008. "The Hidden Side of Invasions: Massive Introgression by Local Genes." *Evolution* 62: 1908–1920.

Danecek, P., A. Auton, G. Abecasis, et al. 2011. "The Variant Call Format and VCFtools." *Bioinformatics* 27: 2156–2158.

Davis, O. K., and R. M. Turner. 1986. "Palynological Evidence for the Historic Expansion of Juniper and Desert Shrubs in Arizona, U.S.A." *Review of Palaeobotany and Palynology* 49: 177–193.

Derryberry, E. P., G. E. Derryberry, J. M. Maley, and R. T. Brumfield. 2014. "HZAR: Hybrid Zone Analysis Using an R Software Package." *Molecular Ecology Resources* 14: 652–663.

Eaton, D. A., and I. Overcast. 2020. "Ipyrad: Interactive Assembly and Analysis of RADseq Datasets." *Bioinformatics* 36: 2592–2594.

Endler, J. A. 1977. *Geographic Variation, Speciation and Clines*. Princeton University Press.

Faria, R., K. Johannesson, R. K. Butlin, and A. M. Westram. 2019. "Evolving Inversions." *Trends in Ecology & Evolution* 34: 239–248.

Flouri, T., X. Jiao, J. Huang, B. Rannala, and Z. Yang. 2023. "Efficient Bayesian Inference Under the Multispecies Coalescent With Migration." *Proceedings of the National Academy of Sciences* 120: e2310708120.

Flouri, T., X. Jiao, B. Rannala, and Z. Yang. 2020. "A Bayesian Implementation of the Multispecies Coalescent Model With Introgression for Phylogenomic Analysis." *Molecular Biology and Evolution* 37: 1211–1223.

Gompert, Z., and C. A. Buerkle. 2011. "Bayesian Estimation of Genomic Clines." *Molecular Ecology* 20: 2111–2127.

Gompert, Z., E. G. Mandeville, and C. A. Buerkle. 2017. "Analysis of Population Genomic Data From Hybrid Zones." *Annual Review of Ecology, Evolution, and Systematics* 48: 207–229.

Harrison, R. G. 1993. *Hybrid Zones and the Evolutionary Process*. Oxford University Press.

Harrison, R. G., and E. L. Larson. 2014. "Hybridization, Introgression, and the Nature of Species Boundaries." *Journal of Heredity* 105: 795–809.

Hillis, D. M., and J. E. Simmons. 1986. "Dynamic Change of a Zone of Parapatry Between Two Species of *Pholidobolus* (Sauria: Gymnophthalmidae)." *Journal of Herpetology* 20: 85–87.

Hoang, D. T., O. Chernomor, A. von Haeseler, B. Q. Minh, and L. S. Vinh. 2018. "UFBoot2: Improving the Ultrafast Bootstrap Approximation." *Molecular Biology and Evolution* 35: 518–522.

Ji, J., D. J. Jackson, A. D. Leaché, and Z. Yang. 2023. "Power of Bayesian and Heuristic Tests to Detect Cross-Species Introgression With Reference to Gene Flow in the *Tamias quadrivittatus* Group of North American Chipmunks." *Systematic Biology* 72: 446–465.

Jiao, X., T. Flouri, and Z. Yang. 2021. "Multispecies Coalescent and Its Applications to Infer Species Phylogenies and Cross-Species Gene Flow." *National Science Review* 8: nwab127.

Jiggins, C. D., and J. Mallet. 2000. "Bimodal Hybrid Zones and Speciation." *Trends in Ecology & Evolution* 15: 250–255.

Kalyaanamoorthy, S., B. Q. Minh, T. K. F. Wong, A. von Haeseler, and L. S. Jermiin. 2017. "ModelFinder: Fast Model Selection for Accurate Phylogenetic Estimates." *Nature Methods* 14: 587–589.

Key, K. H. L. 1968. "The Concept of Stasipatric Speciation." *Systematic Biology* 17: 14–22.

Kirkpatrick, M. 2010. "How and Why Chromosome Inversions Evolve." *PLoS Biology* 8: e1000501.

Leaché, A. D., B. L. Banbury, C. W. Linkem, and A. Nieto-Montes de Oca. 2016. "Phylogenomics of a Rapid Radiation: Is Chromosomal Evolution Linked to Increased Diversification in North American Spiny Lizards (Genus *Sceloporus*)?" *BMC Evolutionary Biology* 16: 1–16.

Leaché, A. D., and C. J. Cole. 2007. "Hybridization Between Multiple Fence Lizard Lineages in an Ecotone: Locally Discordant Variation in Mitochondrial DNA, Chromosomes, and Morphology." *Molecular Ecology* 16: 1035–1054.

Leaché, A. D., J. A. Grummer, R. B. Harris, and I. K. Breckheimer. 2017. "Evidence for Concerted Movement of Nuclear and Mitochondrial Clines in a Lizard Hybrid Zone." *Molecular Ecology* 26: 2306–2316.

Leaché, A. D., and T. W. Reeder. 2002. "Molecular Systematics of the Eastern Fence Lizard (*Sceloporus undulatus*): A Comparison of Parsimony, Likelihood, and Bayesian Approaches." *Systematic Biology* 51: 44–68.

Li, X., O. Sunday Okoh, and N. Sequeira Trovão. 2025. "The Impact of Software and Criteria on the Selection of Best-Fit Nucleotide Substitution Models for Molecular Evolutionary Genetic Analysis." *PLoS One* 20: e0319774.

Li, X. Y., and H. Kokko. 2019. "Sex-Biased Dispersal: A Review of the Theory." *Biological Reviews* 94: 721–736.

Lowe, C. H., and K. S. Norris. 1956. "A subspecies of the lizard Sceloporus undulatus from the White Sands of New Mexico." *Herpetologica* 12, no. 2: 125–127.

Martin, S. H., J. W. Davey, C. Salazar, and C. D. Jiggins. 2019. "Recombination Rate Variation Shapes Barriers to Introgression Across Butterfly Genomes." *PLoS Biology* 17: e2006288.

Martin, S. H., and C. D. Jiggins. 2017. "Interpreting the Genomic Landscape of Introgression." *Current Opinion in Genetics and Development* 47: 69–74.

McEntee, J. P., J. G. Burleigh, and S. Singhal. 2020. "Dispersal Predicts Hybrid Zone Widths Across Animal Diversity: Implications for Species Borders Under Incomplete Reproductive Isolation." *American Naturalist* 196: 9–28.

Miller, R. F., and P. E. Wigand. 1994. "Holocene Changes in Semiarid Pinyon-Juniper Woodlands: Response to Climate, Fire, and Human Activities in the US Great Basin." *Bioscience* 44: 465–474.

Nguyen, L., H. A. Schmidt, A. von Haeseler, and B. Q. Minh. 2015. "IQ-TREE: A Fast and Effective Stochastic Algorithm for Estimating Maximum-Likelihood Phylogenies." *Molecular Biology and Evolution* 32: 268–274.

Okamoto, K., A. Tominaga, and M. Toda. 2024. "Demographic Imbalance in the Hybrid Zone Led to Asymmetric Gene Flow Between Two Closely Related Geckos, *Gekko hokouensis* and *Gekko yakuensis* (Squamata: Gekkonidae)." *Biological Journal of the Linnean Society* 141: 118–132.

Peterson, B. K., J. N. Weber, E. H. Kay, H. S. Fisher, and H. E. Hoekstra. 2012. "Double Digest RADseq: An Inexpensive Method for De Novo SNP Discovery and Genotyping in Model and Non-Model Species." *PLoS One* 7: e37135.

Plummer, M., N. Best, K. Cowles, and K. Vines. 2006. "CODA: Convergence Diagnosis and Output Analysis for MCMC." *R News* 6: 7–11.

Polechová, J., and N. Barton. 2011. "Genetic Drift Widens the Expected Cline but Narrows the Expected Cline Width." *Genetics* 189: 227–235.

Rannala, B., and Z. Yang. 2003. "Bayes Estimation of Species Divergence Times and Ancestral Population Sizes Using DNA Sequences From Multiple Loci." *Genetics* 164: 1645–1656.

Sites, J. W., N. H. Barton, and K. M. Reed. 1995. "The Genetic Structure of a Hybrid Zone Between Two Chromosome Races of the *Sceloporus grammicus* Complex (Sauria, Phrynosomatidae) in Central Mexico." *Evolution* 49: 9–36.

Sloan, D. B., J. C. Havird, and J. Sharbrough. 2017. "The On-Again, Off-Again Relationship Between Mitochondrial Genomes and Species Boundaries." *Molecular Ecology* 26: 2212–2236.

Szymura, J. M., and N. H. Barton. 1986. "Genetic Analysis of a Hybrid Zone Between the Fire-Bellied Toads, *Bombina bombina* and *Bombina variegata*, Near Cracow in Southern Poland." *Evolution* 40: 1141–1159.

Taylor, S. A., E. L. Larson, and R. G. Harrison. 2015. "Hybrid Zones: Windows on Climate Change." *Trends in Ecology & Evolution* 30: 398–406.

Thawornwattana, Y., F. Seixas, Z. Yang, and J. Mallet. 2023. "Major Patterns in the Introgression History of *Heliconius* Butterflies." *eLife* 12: RP90656.

Tinkle, D. W., and A. E. Dunham. 1986. "Comparative Life Histories of Two Syntopic Sceloporine Lizards." *Copeia* 1986: 1–18.

Toews, D. P., and A. Brelsford. 2012. "The Biogeography of Mitochondrial and Nuclear Discordance in Animals." *Molecular Ecology* 21: 3907–3930.

Wielstra, B. 2019. "Historical Hybrid Zone Movement: More Pervasive Than Appreciated." *Journal of Biogeography* 46: 1300–1305.

Supporting Information

Additional supporting information can be found online in the Supporting Information section.